



Published in final edited form as:

Proc SPIE Int Soc Opt Eng. 2017 February 11; 10135: . doi:10.1117/12.2254676.

Evaluation of lung tumor motion management in radiation therapy with dynamic MRI

Seyoun Park¹, Rana Farah¹, Steven M. Shea², Erik Tryggestad³, Russell Hales¹, and Junghoon Lee¹

¹Department of Radiation Oncology and Molecular Radiation Sciences, Johns Hopkins University, Baltimore, MD, USA

²Department of Radiology, Stritch School of Medicine, Loyola University Chicago, Maywood, IL, USA

³Department of Radiation Oncology, Mayo Clinic, Rochester, MN, USA

Abstract

Surrogate-based tumor motion estimation and tracing methods are commonly used in radiotherapy despite the lack of continuous real time 3D tumor and surrogate data. In this study, we propose a method to simultaneously track the tumor and external surrogates with dynamic MRI, which allows us to evaluate their reproducible correlation. Four MRI-compatible fiducials are placed on the patient's chest and upper abdomen, and multi-slice 2D cine MRIs are acquired to capture the lung and whole tumor, followed by two-slice 2D cine MRIs to simultaneously track the tumor and fiducials, all in sagittal orientation. A phase-binned 4D-MRI is first reconstructed from multi-slice MR images using body area as a respiratory surrogate and group-wise registration. The 4D-MRI provides 3D template volumes for different breathing phases. 3D tumor position is calculated by 3D-2D template matching in which 3D tumor templates in 4D-MRI reconstruction and the 2D cine MRIs from the two-slice tracking dataset are registered. 3D trajectories of the external surrogates are derived via matching a 3D geometrical model to the fiducial segmentations on the 2D cine MRIs. We tested our method on five lung cancer patients. Internal target volume from 4D-CT showed average sensitivity of 86.5% compared to the actual tumor motion for 5 min. 3D tumor motion correlated with the external surrogate signal, but showed a noticeable phase mismatch. The 3D tumor trajectory showed significant cycle-to-cycle variation, while the external surrogate was not sensitive enough to capture such variations. Additionally, there was significant phase mismatch between surrogate signals obtained from fiducials at different locations.

Keywords

Dynamic MRI; lung cancer; motion management; radiation therapy

1. Introduction

Respiration-induced tumor motion is a major obstacle for achieving high-precision radiotherapy of cancers in the thorax and abdomen. Common motion management strategies currently used in radiotherapy include respiration gating, real-time tumor tracking, and breath-hold techniques where external or internal surrogates are typically used to derive the

patient and tumor position [1-4]. While these methods may yield an improved treatment with reduced margins, they have inherent limitations. Tracking techniques often expose patients to ionizing radiation. Additionally, an invasive procedure may be necessary for internal surrogate marker placement. Anatomic motion due to breathing is significantly variable between breathing cycles, treatment fractions, individual patients, tumor location, and sometimes shows complex patterns [5-6]. Tumor motion management strategies are recommended for quality care by national treatment guidelines in radiation oncology [7]. However, an understanding of the uncertainty behind surrogate-based motion management strategies is limited.

Computed tomography (CT) is the reference imaging modality for radiotherapy planning and dose computation. Accordingly, respiration-correlated CT or 4D-CT is considered an effective tool to characterize tumor and normal tissue motion during radiotherapy. 4D-CT has become the gold standard for radiotherapy treatment planning in the context of breathing motion, and a pre-treatment 4D-CT scan is typically obtained to derive internal target motion for radiotherapy planning. However, it is often overlooked that 4D-CT is a snapshot representation of a single-breathing cycle. Additionally, CT deposits additional radiation dose to the patient, thus hindering its applicability in acquiring information over timescales consistent with a treatment session.

Magnetic resonance imaging (MRI) is advantageous due to its capability of visualizing target tumor in contextual anatomy with excellent soft tissue contrast. MRI poses minimal risk to patients because it is non-ionizing, making it highly suitable for longer duration and repeated scans. Recent advances in dynamic MR imaging technologies enable MRI-guided radiation therapy [8], which may better characterize organ motion. Dynamic MRI can improve 4D radiation therapy by giving continuous, rather than sparse data on tumor motion throughout a prolonged period of respiratory movement, during a single treatment session or a course of radiation treatment.

There have been studies to track tumor motion with 2D cine MR images [4, 9, 10]. However, only a few groups have analyzed the correlation between the tumor motion and surrogate using 2D dynamic MR imaging techniques [4, 10], and none of them directly imaged the tumor and the external surrogate simultaneously. In this study, we propose a method to simultaneously track the 3D position of the tumor and external surrogates with dynamic MRI, which allows us to evaluate the correlation between the tumor motion and external surrogate signal for radiation therapy.

2. Methods

After informed consent was obtained, newly diagnosed lung cancer patients were enrolled on a IRB based research protocol to assess tumor versus surrogate motion using 4D MRI. MRI used for this study were obtained prior to therapy. To simultaneously track 3D tumor and external fiducial motions, we acquired 2D multi-slice and two-slice sagittal cine MR images. The sagittal orientation is preferred because the target tumor and surrogate motion is mainly along superior-inferior (SI) and anterior-posterior (AP) directions with much smaller lateral motion. Multi-slice MRI allows for reconstruction to a 4D-MRI, which provides a

representation of the tumor motion that is largely analogous to 4D-CT. However, this representative 4D-MRI does not provide actual (or real time) 3D tumor and fiducial motion information. To simultaneously track both tumor and surrogate motion, a two-slice 2D cine MR scan is performed. In this scan, one slice is positioned to capture both the tumor and two fiducials located on the tumor side, while the other slice is positioned to capture the remaining two fiducials on the non-tumor side as shown in Figure 1(d).

2.1 4D-MRI reconstruction and tumor template

To obtain tumor template volumes at different breathing phases, we first reconstruct 4D-MRI from the multi-slice MR images. The patient's respiratory signal is extracted by computing body area on each 2D image [11]. Each respiration cycle is divided into 10 breathing phase, and the collected multi-slice MR images are sorted into these 10 breathing phases. Each phase bin contains multiple MR images that are at the same breathing phase but with variations due to uncertainties in phase binning. Therefore, we perform group-wise registration between sorted images in the same bin to reconstruct a 2D image at each slice location in particular breathing phase [12, 13]. We repeat this reconstruction process across different slice locations and breathing phases. The reconstructed slices at each breathing phase are then stacked to form a 3D reconstructed volume. The final outcome is a series of 10 reconstructed volumes, each representing a 3D volume per breathing phase. Tumor volumes are manually segmented from the 4D-MRI reconstruction and serve as the reference templates for 3D tumor motion tracking in the next step.

2.2 Tumor tracking

3D tumor motion is estimated from the two-slice cine MRIs in which tumor is captured in one of the two slices. We estimate the 3D motion from the 2D scan by 3D (tumor template in 4D-MRI) to 2D (cine MRI) registration. The sequential 2D cine MR images are sorted by the same phase-binning approach used for 4D-MRI reconstruction, and a rigid transformation from the 3D tumor template in the same phase to the target 2D image is estimated by maximizing normalized cross-correlation (NCC) on the 2D MR image plane. We use the quasi-Newton method to find the optimal solution, and six parameters including xyz -translation and Euler angles are estimated.

2.3 Fiducial tracking

The MRI-compatible fiducial designed for our study consists of four cylinders filled with 0.9% sodium chloride normal saline which have high signal intensity for the MR pulse sequence. They are mounted on top and bottom side of a V-shaped acrylic body (Figure 2a and b) with a dimension of $8.2 \times 7.6 \times 2.4 \text{ cm}^3$ (width \times height \times thickness). When imaged in a sagittal view in our scan setting, it produces a unique 2D slice print as shown in Figure 2(c). The 3D motion of the fiducial is calculated by matching its 3D geometrical model to 2D cine images. A 3D geometrical model of the fiducial was derived from its CT scan where center lines of the four cylinders and centroid of the fiducial body are computed. In 2D MR image, four fiducials are clearly shown and automatically segmented and indexed.

The line segment connecting two end point $\mathbf{p}, \mathbf{q} \in \mathbb{R}^3$ can be written in parametric form $\mathbf{l}(t) = \mathbf{x} = \mathbf{p} + (\mathbf{q} - \mathbf{p})t$ ($0 \leq t \leq 1$). Since there are 4 cylinders in a fiducial, the fiducial geometry can

be defined by an ordered set of four line segments $\mathbf{F}=(\mathbf{l}_1, \mathbf{l}_2, \mathbf{l}_3, \mathbf{l}_4)$. Because the fiducial is shown as bright circles in MR images as shown in Figure 2(c), they are segmented by thresholding and morphological filtering and indexed by their locations automatically. The fiducial tracking problem becomes a rigid registration problem and can be solved by fitting the fiducial model \mathbf{F} to their segmentations in the MR images. The image plane is defined as $\mathbf{n} \cdot (\mathbf{x} - \mathbf{o}) = 0$, where \mathbf{o} is the offset and \mathbf{n} is the normal vector. The intersection point \mathbf{x} between the line segment and the plane can be computed by

$$\mathbf{x} = \mathbf{p} + \frac{\mathbf{n} \cdot (\mathbf{o} - \mathbf{p})}{\mathbf{n} \cdot \mathbf{d}} \mathbf{d} = \frac{(\mathbf{n} \cdot \mathbf{o})\mathbf{d} + \mathbf{n} \times (\mathbf{p} \times \mathbf{d})}{\mathbf{n} \cdot \mathbf{d}} \quad (1)$$

where $\mathbf{d} = \mathbf{q} - \mathbf{p} / \|\mathbf{q} - \mathbf{p}\|$. Let $T(\mathbf{x}): \mathbb{R}^3 \rightarrow \mathbb{R}^3$ be the rigid transformation of the line segment to the image plane. To estimate the 3D center of the fiducial markers from the 2D MR images, we find the optimal transformation which minimizes the cost function defined as

$$\sum_{i=1}^4 \|\mathbf{c}_i - T(\mathbf{x}_i)\|^2 \quad (2)$$

where \mathbf{c}_i is the center of the segmented marker in 2D MRI as shown in Figure 2(c) and

$$T(\mathbf{x}) = \frac{(\mathbf{n} \cdot \mathbf{o})T(\mathbf{d}) + \mathbf{n} \times (T(\mathbf{p}) \times T(\mathbf{d}))}{\mathbf{n} \cdot T(\mathbf{d})} \quad (3)$$

The rigid transformation T is a parametric function of xyz -translation and Euler angles in our model, and (2) becomes a non-linear least squares problem of the parameters. To find an optimal solution, we use the well-known Levenberg-Marquardt algorithm, and the initial solution is estimated from the trapezoidal geometry of the fiducial image in the 2D MR images. Finally, the fiducial centroid trajectory of each fiducial is computed based on the estimated transformation, yielding a surrogate signal.

3. Results

We tested our method on five lung cancer patients. All MR images are acquired using Siemens Magnetom Espree 1.5T scanner (Siemens Medical Solutions, Malvern, PA) with a balanced steady-state free precession sequence (TrueFISP, $TR \approx 3$ ms, $TE = 1.22$ ms, flip angle = $77-79^\circ$). Acquired images were corrected for geometric distortion using the Siemens distortion correction algorithm implemented in the Syngo platform (Siemens AG, Erlangen, Germany). The obtained 2D MR images have a spatial resolution of 2×2 mm² with slice thickness and spacing of 5 mm. The slice acquisition frequency was approximately 4 Hz on average. The number of slices in multi-slice MR scan varied between 15 and 20 depending

on the tumor size. Total scan times were 10 minutes for multi-slice MRI and 5 minutes for two-slice MRI.

Figure 3 shows two examples of the tumor and surrogate signal comparison. In all five lung cancer cases, the tumor motion was correlated with the surrogate signal estimated from fiducials in general as shown in Figure 3(a), but often showed significant phase mismatch as shown in Figure 3(b). The phase mismatch was not systematic, but transient, which may pose significant problem in external surrogate-based tumor motion tracking during radiotherapy. Additionally, there were significant tumor trajectory variations depending on the patient's breathing pattern that were not properly captured by the surrogate signals. We also observed that there was significant phase difference between the upper and lower fiducials. This is due to the variation of the surface motion around the upper and lower (close to abdomen) chest areas depending on breathing patterns. This implies that the position of the external fiducial should be chosen with caution. Also, tumor locations cause different patterns of mismatches between the tumor motion and the surrogate signals. Therefore, tumor locations also have to be considered with care when estimating their motion based on surrogate signals.

The overall phase difference between the tumor and fiducial motions are shown in Table 1. Since lateral motion was very small for these cases, we only show superior-inferior (SI) and anterior-posterior (AP) directional motions in this table. Notice that for some cases, e.g., cases 2 and 3, there are significant phase mismatches between the tumor and fiducial signals. In such instances, surrogate signal based motion management will be inaccurate. Additionally, the assessment results for five cases show that, on average, the sensitivity of ITV was 86.5 % and 43.8% of the volume within ITV was normal tissue. The sensitivity of ITV is the volume percentage of tumor (GTV) included in ITV. The sensitivity is computed at every time frame and the mean and standard deviations are computed for all 5 minutes as shown in Table 1.

4. Conclusions

We proposed a novel method to track tumor and external fiducial motions with dynamic MRI. Based on our development, we qualitatively and quantitatively compared the external surrogate signals and ITV to actual tumor motion. Our preliminary results indicate that the external surrogate-based tumor motion estimation may not be an accurate way to manage the tumor motion during radiotherapy. These data suggests that a surrogate-based tumor motion management strategy during radiation therapy should be used with caution. More extensive evaluation on a larger patient cohort is underway.

Acknowledgments

This work was supported by NIH/NCI under the grant R21CA178455.

References

1. Mah D, Hanley J, Rosenzweig KE, Yorke E, Braban L, Ling CC, Mageras G. Technical aspects of the deepinspiration breath hold technique in the treatment of thoracic cancer. *International Journal of Radiation Oncology, Biology, Physics*. 2000; 48:1175–1185.

2. Wong JW, Sharpe MB, Jaffray DA, Kini VR, Robertson JM, Stromberg JS, Martinez AA. The use of active breathing control (ABC) to reduce margin for breathing motion. *International Journal of Radiation Oncology, Biology, Physics*. 1999; 44(4):911–919.
3. Berbeco RI, Nishioka S, Shirato H, Chen GT, Jiang SB. Residual motion of lung tumours in gated radiotherapy with external respiratory surrogates. *Physics in Medicine and Biology*. 2005; 50:3655–3667. [PubMed: 16077219]
4. Paganelli C, et al. Magnetic resonance imaging-guided versus surrogate-based motion tracking in liver radiation therapy: A prospective comparative study. *International Journal of Radiation Oncology, Biology, Physics*. 2015; 91(4):840–848.
5. Bruce EN. Temporal variations in the pattern of breathing. *Journal of Applied Physiology*. 1996; 80:1079–1087.
6. Hoisak J, Sixel K, Tirona R, Cheung P, Pignol JP. Prediction of lung tumour position based on spirometry and on abdominal displacement: Accuracy and reproducibility. *Radiotherapy and Oncology*. 2006; 78:339–346. [PubMed: 16537094]
7. Ettinger D, et al. NCCN guidelines insights: Non-small cell lung cancer, version 4.2016. *Journal of the National Comprehensive Cancer Network*. 2016; 14(3):255–264. [PubMed: 26957612]
8. Bjerre T, Crijs S, afRosenschold PM, Aznar M, Specht L, Larsen R, Keall P. 3D MRI-linac intra-fraction guidance using multiple orthogonal cine MRI planes. *Physics in Medicine & Biology*. 2013; 58:4943–4950. [PubMed: 23807514]
9. Tryggestad E, Flammang A, Hales R, Herman J, Lee J, McNutt T, Roland T, Shea SM, Wong J. 4D tumor centroid tracking using orthogonal 2D dynamic MRI: Implications for radiotherapy planning. *Medical Physics*. 2013; 40(9):091712. [PubMed: 24007145]
10. Feng M, Balter JM, Normolle D, Adusumilli S, Cao Y, Chenevert TL, Ben-Josef E. Characterization of pancreatic tumor motion using cine MRI: surrogates for tumor position should be used with caution. *International Journal of Radiation Oncology, Biology, Physics*. 2007; 52:N401–15.
11. Liu Y, Yin FF, Chang Z, Czito BG, Palta M, Bashir MR, Qin Y, Cai J. Investigation of sagittal image acquisition for 4D-MRI with body area as respiratory surrogate. *The International Journal of Medical Physics Research and Practice*. 2014; 41(10)
12. Farah R, Shea S, Tryggestad E, Forbang RT, Wong J, Hales R, Lee J. 4D-MRI reconstruction using group-wise registration. *Medical Physics*. 2015; 42(6):3737.
13. Farah R, Park S, Shea S, Tryggestad E, Wong J, Hales R, Lee J. Evaluation of lung tumor motion management strategy with dynamic MRI. *Medical Physics*. 2016; 43(6):3879.

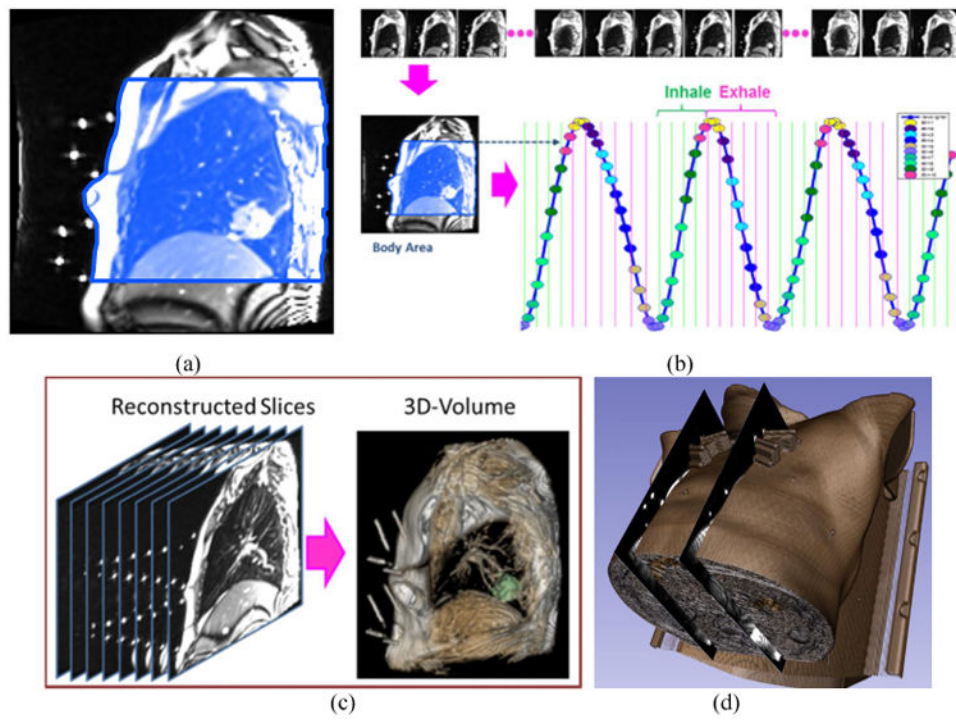


Figure 1. Dynamic MR image acquisition and tumor tracking. (a) Body area computation for respiratory signal. (b) Phase binning. (c) 4D-MRI reconstruction and tumor segmentation. (d) 2D dynamic cine MR acquisition. 3D rendering of the two fiducials placed on the chest are overlaid and MR images of the other two fiducials on the abdomen are shown.

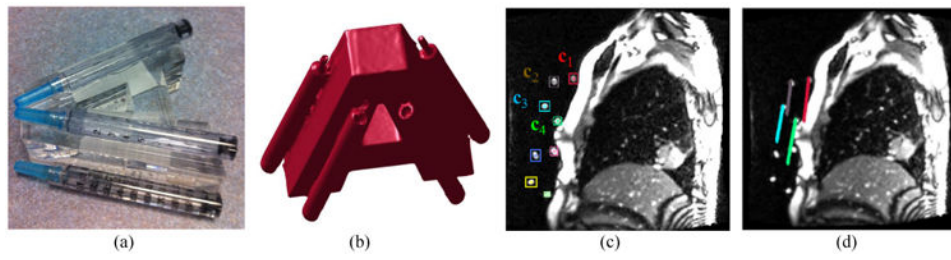


Figure 2. Fiducial tracking. (a) MRI-compatible fiducial. (b) CT scan for modeling. (c) Fiducial segmentation in 2D MR image. (d) 3D fiducial tracking.

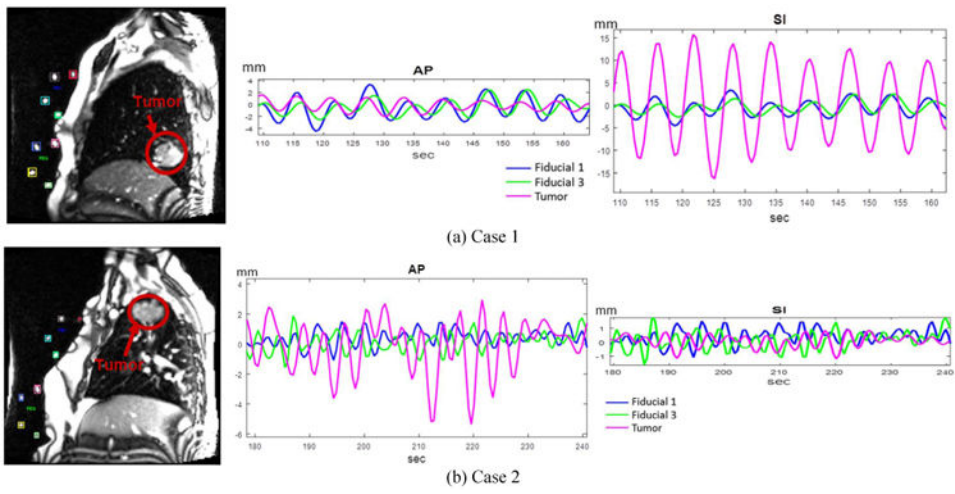


Figure 3.
Tumor motion and surrogate signals estimated from the fiducials.

Comparison between tumor and fiducial motions, and assessment of the sensitivity and normal tissue inclusion for ITV approach.

Table 1

	ITV comparison (%)		Phase difference in seconds (mean \pm standard deviation)				Tumor motion
	Sensitivity	Normal tissue	Fiducial 1	Fiducial 2	Fiducial 3	Fiducial 4	
Case 01	82.4 \pm 10.7	53.1 \pm 6.1	0.043 \pm 0.14 0.301 \pm 0.29	0.108 \pm 0.21 0.215 \pm 0.39	0.108 \pm 0.21 0.452 \pm 0.47	0.409 \pm 0.44 0.925 \pm 0.54	SI AP
Case 02	89.1 \pm 5.5	38.2 \pm 7.4	0.559 \pm 0.47 0.999 \pm 0.74	0.655 \pm 0.55 0.942 \pm 0.80	0.575 \pm 0.52 0.747 \pm 0.52	0.607 \pm 0.58 0.878 \pm 0.81	SI AP
Case 03	88.3 \pm 6.4	39.6 \pm 6.3	0.763 \pm 0.72 0.603 \pm 0.67	0.634 \pm 0.69 0.587 \pm 0.56	0.699 \pm 0.72 0.604 \pm 0.58	0.826 \pm 0.79 0.731 \pm 0.74	SI AP
Case 04	87.9 \pm 8.3	43.9 \pm 8.4	0.447 \pm 0.63 0.575 \pm 0.54	0.447 \pm 0.48 0.543 \pm 0.60	0.591 \pm 0.63 0.543 \pm 0.60	0.607 \pm 0.68 0.583 \pm 0.60	SI AP
Case 05	85.6 \pm 9.4	44.2 \pm 5.6	0.247 \pm 0.33 0.375 \pm 0.42	0.314 \pm 0.31 0.319 \pm 0.40	0.359 \pm 0.43 0.451 \pm 0.40	0.507 \pm 0.48 0.531 \pm 0.52	SI AP